Preprints of the 21st IFAC World Congress (Virtual)
Berlin, Germany, July 12-17, 2020

Recent Results in Reference Prefiltering for Precision Motion Control

Tarunraj Singh * **Tomáš Vyhlídal** **

* *Department of Mechanical & Aerospace Engineering University at Buffalo, Buffalo, NY 14260, USA e-mail: tsingh@buffalo.edu.*
** *Department of Instrumentation and Control Engineering, and Center of Advanced Aerospace Technology, Faculty of Mechanical Engineering, Czech Technical University in Prague, Czechia, e-mail: tomas.vyhlidal@fs.cvut.cz*

Abstract: Input Shaping/Time-Delay Filtering is now an established approach for shaping reference inputs to minimize residual vibrations for rest-to-rest maneuvers, velocity and periodic tracking controllers, and to minimize excitation of high frequency unmodelled modes. At the core of successful reference shaping approaches have been the encapsulation of robustness to model parameter uncertainties. Special attention has also been paid to incorporation of the input shapers within closed loops of various configurations. This paper reviews existing designs for input shaping and highlights some of the latest contributions related to input shaping for precision motion control.

Keywords: Input Shaping, Time-Delay Filters, Reference Shaping, Motion Control, Vibration Control, Path Planning of Underdamped Systems, Rest-to-Rest maneuvers

1. INTRODUCTION

Vibration mitigation of lightly damped structures including flexible arm robots, atomic force microscopes, hard disk drives, cranes etc. has drawn attention over the past few decades. The demand for faster and lighter mechanisms in various applications has resulted in the design of underdamped structures whose motion induced vibrations need to be mitigated to realize the benefit of the lightweight structure. Building on the pioneering work by Smith (1958) (Posicast control), Singer and Seering (1990)'s concept of Input Shaping reignited the interest of the control community on the use of filtering to shape the reference input to a stable system. Over the past three decades, this renewed interest has resulted in a vast body of literature on precision motion control of vibratory systems (Singh and Singhose (2002); Singhose (2009); Singh (2009)).

Before addressing the selected aspects in reference prefiltering for precision motion control by input shapers, let us outline the fundamentals of the problem at hand. A classical feed-forward interconnection of an input shaper and the controlled flexible system is shown in Fig. 1. The purpose of the shaper is to shape the reference r in order to pre-compensate the oscillatory modes of the flexible subsystem $F(s)$, given by the damping and natural frequencies $\xi_i, \omega_i, i = 1 \dots m$. Note that for successful mode compensation in the scheme in Fig. 1, the closed loop actuator dynamics $\frac{C(s)G(s)}{1+C(s)G(s)}$ need to be sufficiently fast compared to the modes of $F(s)$ to be compensated.

In general, the shaper is considered in the form

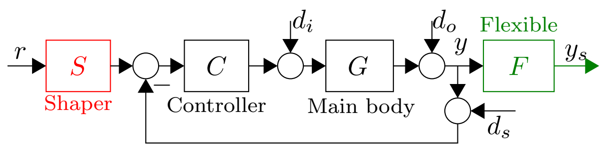

Fig. 1. Feedforward interconnection of a reference shaper

$$u(t) = A_0 r(t) + \sum_{i=1}^{n} A_i r(t - \tau_i), \tag{1}$$

where r, u are the input and the output of the shaper, respectively, $A_i \in [0, 1], i = 0 \dots n$ are the gains and τ_i are the lumped time delays satisfying $0 < \tau_1 < ... < \tau_n$. In order to keep the unity gain of the shaper, the coefficients $A_i, i = 0 \dots n$ need to satisfy the equality

$$\sum_{i=0}^{n} A_i = 1. \tag{2}$$

Let us note that for the Smith's Posicast, a single oscillatory mode ($m = 1$) is to be targeted with (1), $n = 1$, which is identical with zero-vibration (ZV) shaper (Singer and Seering (1988, 1990); Singhose et al. (1994)) given by

$$u(t) = A_0 r(t) + A_1 r(t - \tau_1). \tag{3}$$

The transfer function of the shaper (1) is given as

$$S(s) = A_0 + \sum_{i=1}^{n} A_i \mathrm{e}^{-s\tau_i}. \tag{4}$$

If the i^{th}−root underdamped mode: $r_i = -\xi_i\omega_i - j\omega_i\sqrt{1-\xi_i^2}$ (and the complex conjugate root) is to be fully compensated, the following equation needs to be satisfied

$$S(r_i) = 0. \tag{5}$$

Thus, from the spectral point of view, the functioning of the shaper is achieved by direct *shaper-zero - system-pole* compensation.

An alternative design strategy of the input shaper is via the residual vibration function

$$V(\omega,\xi) = \mathrm{e}^{-\xi\omega\tau_n}\sqrt{R(\omega,\xi)^2 + I(\omega,\xi)^2} \tag{6}$$

where

$$R(\omega,\xi) = A_0 + \sum_{i=1}^{n} A_i \mathrm{e}^{\xi\omega\tau_i}\cos(\omega\sqrt{1-\xi^2}\tau_i) \tag{7}$$

$$I(\omega,\xi) = \sum_{i=1}^{n} A_i \mathrm{e}^{\xi\omega\tau}\sin(\omega\sqrt{1-\xi^2}\tau_i), \tag{8}$$

determining the scaled amplitude of the residual vibrations at time $t = t_n$, Singer and Seering (1990), Singhose et al. (1994). The design counterpart to (5) is given by

$$V(\omega_i,\xi_i) = 0. \tag{9}$$

Let us also mention that the residual vibration function is linked to a transfer function (4) frequency response

$$V(\omega,\xi) = \left|S(-\xi\omega - j\omega\sqrt{1-\xi^2})\right|\mathrm{e}^{\xi\omega\tau_n}. \tag{10}$$

Satisfying only this requirement leads to ZV shaper with the residual vibration function visualised in Fig. 2

Application of the residual vibration measure $V(\omega_i,\xi_i)$ is beneficial from the robustness analysis point of view, taking into account the mismatch between the design and true dynamical modes to be compensated. As will be discussed in more detail further, the robustness can be imposed by reducing $V(\omega,\xi)$ in the local neighbourhood of the flexible mode (ξ_i,ω_i), either analytically or numerically - see the ZVD, ZVDD and EI characteristics in Fig. 2.

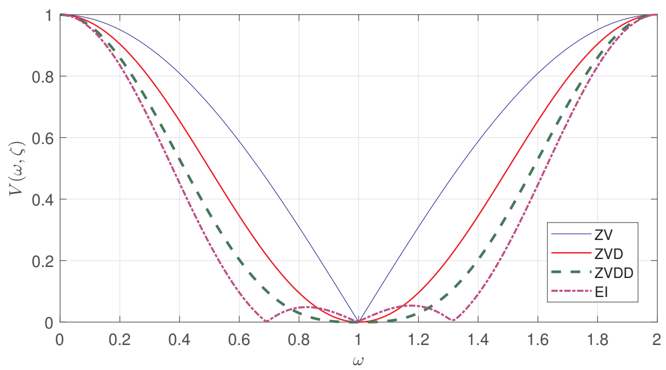

Fig. 2. Residual vibration various input shapers

1.1 *Distributed delay shapers and discrete-time FIR filters*

Next to the input shaping, various command profiles, e.g. Trapezoidal and S-curve function, are used to smooth the rapid changes in the reference or input signals of flexible systems, and thus to decrease the vibrations, Meckl and Arestides (1998). As shown in Singhose et al. (2010), the input shaping is a considerably faster and more efficient technique for reducing vibrations compared to the command smoothing. A partial advantage of the smoothers is filtration at the high frequency range. The properties of input shapers and smoothers have been merged recently by introducing the distributed delay input shapers, Vyhlídal et al. (2013), Alikoç et al. (2016).

Utilizing the Stieltjes integral, both the lumped delay shaper (1) and the distributed delay shaper can be described by

$$u(t) = A_0 r(t) + (1 - A_0)\int_0^T r(t-\eta)dh(\eta) \tag{11}$$

where T is the overall delay length and $h(\eta)$ is the distribution of the delay. For the lumped delay shaper (1), $h(\eta)$ is a step-wise function with weighted steps at τ_i and $T = \tau_n$. For the distributed delay ZV (DZV) shaper introduced in Vyhlídal et al. (2013), the delay distribution function is given by $h(\eta) = \frac{1}{T}\eta, \eta \in [0,T]$. In Vyhlídal and Hromčík (2015), various distributions of the delay were proposed and tested, S-curve, trigonometric and triangular distribution, in particular. Next to smoothing the response at its settling stage, the positive feature of distributed delay shapers are their retarded spectrum of zeros. In particular, the distribution of shaper zeros is important when the shaper is placed within a control loop, Vyhlídal et al. (2016).

Let us note that after discretization of the distributed delay shaper, it can be implemented in the form

$$u(k) = \sum_{i=0}^{n}\bar{A}_i r((k-i)\Delta t), \tag{12}$$

with k denoting the discrete time and Δt the sampling period. Notice that when considering τ_i being equidistantly distributed so that $\tau_i - \tau_{i-1} = \Delta t, i = 1\ldots n$, (12) is formally identical to (1). Notice also that the shaper (12) is in a form of a discrete finite impulse response (FIR), considered e.g. by Singh and Vadali (1995), Cole (2011), Cole and Wongratanaphisan (2011). Thus, the properties of the distributed delay shaper are close to the properties of a FIR-shaper. However, a considerable lower number of parameters is needed as a rule for (11) compared to FIR filter in a form (12). An alternative discrete form of the distributed delay shaper is based on its implementation in a form of a dynamical system, Pilbauer et al. (2017).

After introduction and brief preliminaries, the main part of paper is organised as follows. Section 2 discusses robust shaper design based on nominal models. This is followed by Section 3 which focuses on interval uncertainty based design. This includes legacy and recent designs based on lumped and distributed delays. The following Section 4 discusses recent results in risk based design which exploits probability density function characterization of model parameter uncertainties. This is followed in Section 5 with a brief discussion of recent results on including input shapers within feedback loops. The paper concludes with some thoughts on open problems to pursue in the domain of reference prefiltering and the related problem of including shapers within loops.

2. ROBUST DESIGN BASED ON NOMINAL MODELS

It was noted in the early work of Tallman and Smith (1958) that the model based *Posicast* control approach was sensitive to incorrect estimates of the damping ratio and the natural frequency of the underdamped second order system. After being essentially dormant as a widely studied approach for three decades, the *Posicast* control which is essentially a tap-delay filter saw renewed interest after the inspired formulation of the concept of *Input Shaper* by Singer and Seering (1990). The design of the *Input Shaper* was posed as an optimization problem to determine the amplitude and delay sequence of a series of impulses with the objective of a quiescent response at the end of the impulse sequence, and the additional constraint that the sensitivity of the response of an underdamped second order system to the damping ratio or natural frequency be forced to zero. It was also demonstrated that the sensitivity of the system response to the damping ratio was identical to that to the natural frequency. This corresponded to a concurrent reduction of sensitivity of the response to uncertain estimates in the damping ratio and natural frequency around the nominal estimates of those parameters. This impulse sequence designed to force the vibration at the end of the impulse sequence was called a zero vibration (ZV) *ZV Input Shaper* (given by (3), i.e. $S(s) = A_0 + A_1 \mathrm{e}^{-s\tau_1}$). The impulse sequence which forced the vibration and the gradient of the vibration at the end of the impulse sequence was called a Zero Vibration Derivative (ZVD) Input Shaper. This impulse sequence when convolved with any reference input resulted in a shaped reference profile which eliminated or profoundly reduced the residual vibration relative to the unshaped reference input at the end of the impulse sequence. Singhose et al. (1994) graphically illustrated the fundamental way the Input Shaper results in zero vibration at the end of the impulse sequence. They also presented a graphical interpretation of the ZVD shaper using a phasor.

Singh and Vadali (1993) illustrated that the ZV was identical to a time-delay filter whose amplitudes and delays were selected such that the zeros of the transfer function of the time-delay filter cancelled the underdamped poles of the system. A cascade of two of the time-delay filters designed to cancel the underdamped poles resulted in a ZVD shaper. This also corresponded to locating multiple zeros of the time-delay filter at the nominal location of the poles underdamped system. Increasing the number of zeros of the time-delay filter at the nominal location of the poles of the system increased the robustness of the Input Shaper for perturbations of the system model around the nominal parameters as illustrated in Figure 2 by the flattened curve in the proximity of ω=1 for the ZVD and ZVDD shaper. The EI shaper can be associated with locating multiple zeros around the nominal modes. A prefilter to cancel multiple distinct poles of the underdamped system could be synthesized by cascading multiple time-delay filters, each designed for one mode. Singh and Vadali (1995), Tuttle and Seering (1994) and Murphy and Watanabe (1992) presented techniques for pole-zero cancellation based design of Input Shapers in the continuous and discrete domain respectively, where the filter could be concurrently designed to cancel all the underdamped modes with the fewest delays necessary. Singh and Vadali (1995) also presented a simple approach to design Input-Shapers where the user could select the magnitude of the delays permitting the continuous time design in the discrete time framework.

This concept of locating multiple zeros of the time-delay filter at the nominal location of the poles of the system was used to generate Input Shapers which did not result in a staircase reference profile when driven by a step input. Imposing constraints on the jerk resulted in prefiltered profiles, Singh (2004), which minimized the energy of the shaped profiles in the high frequency domain, resulting in reduced excitation of high frequency unmodelled dynamics. This idea was also used to design a variety of robust open loop optimal control profiles which minimized the maneuver time, Singh and Vadali (1994), fuel-time cost, Hartmann and Singh (1999), fuel limited maneuver time, Singhose et al. (1999), jerk limited maneuver time, Muenchhof and Singh (2003), etc.

The basic concept of Input Shaper design was reduced to cancelling the poles of the underdamped system with the zeros of the time-delay filter. This prompts the obvious question of shaping the reference input to account for the zeros of the input-output transger function of the underdamped system. Perez and Devasia (2003); Iamratanakul et al. (2008) in multiple articles introduced the concept of pre- and post-actuation for output-to-ouput transition of systems and demonstrated improved transition performance relative to control profile without pre- and post-actuation for a class of systems. Singh (2012) posed the design of Input Shapers where the time-delay filter cancelled the underdamped poles as well as the zeros of the system and for systems with minimum-phase zeros resulted in post-actuated control. Non-minimum phase zeros result in pre-actuation shaped profiles. Butterworth et al. (2012) compared three inverse-model approaches for shaping reference inputs in the discrete time domain. They include the the zero-phase-error tracking controller (ZPETC) Tomizuka (1987), nonminimum-phase zeros ignore (NPZ-Ignore), and the zero-magnitude-error tracking controller (ZMETC) Al-Numay (2007). These discrete time approaches also deal with pole-zero, zero-pole cancellations for minimum-phase poles and zeros.

All the aforementioned approaches for design of prefilters to attenuate residual vibration of underdamped systems only required knowledge of the nominal underdamped poles of the system. Robustness was achieved by desensitizing the system response in the proximity of the nominal poles of the system. It should be noted that the robustness is achieved at a cost of increased maneuver time.

Singh (2008) used the residual energy evaluated at the largest delay of the time-delay filter, which is composed of the kinetic energy and a pseudo-potential energy (which is zero when the system displacement is coincident with the desired final value) to design Input Shapers. The issue of robustness was addressed by increasing the order of the system by including the differential equations which represent the sensitivity of the system states to model parameter uncertainties and forcing these sensitivity states to zero at the end of the maneuver Liu and Singh (1997).

A vector based general parametrization procedure of all equidistant four-pulse robust shaping filters with minimum set of chosen parameters was proposed in Schlegel and Goubej (2010). Peng et al. (2019), used the feed-forward smoother in combination with the frequency estimator to reduce both the swing and twisting of the payloads during slewing motions by tower cranes. In Newman et al. (2018), the oscillations induced e.g. by parametric uncertainty or force disturbances are turned to initial condition problem and targeted by the input shaper designed in the time domain.

3. INTERVAL UNCERTAINTIES BASED DESIGN

This section will focus on robust input shaper design given knowledge of the domain of uncertainties. Various cost function which include the 1, 2 and ∞ norm of the residual energy sampled over the uncertain domain, are considered in the shaper design.

3.1 Worst Case Design (∞ norm)

The first effort at requiring a measure of the system response at the end of the Input Shaper's transition be below a specified threshold was addressed via the Extra Insensitive Input Shaper design, Singhose et al. (1994). In this design, the user specifies a tolerable residual vibration for the nominal model, and the optimizer determines two neighboring values of the uncertain parameter where the residual vibration is forced to zero. This expands the domain of the uncertain variable where the residual vibration is below a specified threshold, relative to the ZVD Input Shaper (Figure 2), for the same number of impulse sequence. A complementary approach is called Specified-Insensitivity (SI) shaping, Singhose et al. (1996), where the uncertain parameter is sampled over the specified range of interest, and the residual vibration is minimized over that domain. The exact SI shaper was designed by requiring the residual vibration to equal the tolerable threshold and forcing the slope of the sensitivity curve to zero at a set of unknown frequencies and forcing the residual vibrations to zero at another set of unknown frequencies.

Singh (2002) proposed a minimax optimization problem where the residual energy (kinetic energy plus psuedo-potential energy) at the end of the maneuver is the cost function. The worst cost, i.e., the maximum magnitude of the cost over the domain of uncertainty is minimized by the parameters of the Input Shaper (time-delay filter). This formulation did not require any constraints to be enforced such as the cost being forced to zero at specific realizations of the uncertain parameters. The problem however, did require the uncertain domain to be discretely sampled. A uniform grid of sampling points were selected to solve this problem. This minimax problem is a nonlinear programming problem which is burdened by the fact that the optimal solution might not converge to the global optima. To address this issue, Conord and Singh (2006) posed a Linear Matrix Inequality (LMI) based convex optimization problem which ensures that the resulting solution is near global-optimal. This results from the fact that the LMI based approach also requires sampling of the uncertain domain and as the sampling density increases, the solution will tend to the global-optima.

3.2 Optimal design of input shapers with lumped and distributed delays

In input shaper design, various aspects such as robustness, time response and spectral features are to be handled simultaneously. Taking into account the structural requirements, the design task can be formulated as a standard constrained optimization task. The pioneering work in this subject is Lim et al. (1999), where the shaper is considered in the standard FIR form. The objective of the formulated optimization task is to minimize the number of impulses to track the reference without the residual vibrations. The task is formulated and solved as l_1-norm constrained quasi-convex optimization problem. A multi-level optimization approach for creating discrete time shapers was proposed by Robertson and Singhose (2001). Next to zeroing the residual vibrations for the given frequency, secondary constraints such as robustness, rise time, or number of impulses were targeted by the multi-stage algorithm. Building up on these results, it was shown by Baumgart and Pao (2007) that a feasible discrete-time single-input shaper always exists, considering also a class of MIMO systems.

When both the delays and the gains within the input shaper are to be optimized, it forms a *nonlinear optimization problem*, which is difficult to solve. However, as recognized by Singh and Vadali (1995) and Van den Broeck et al. (2008), once the time delays in the shaper are prefixed, the optimization task is considerably simplified. Instead of several delays considered in the conventional input shaper, its active time range is divided into a large number of equally distributed time samples. The gains taken in these samples then form the parameter set to be optimized. Once the objective function is linear in the gain parameters, the optimization task can be formulated as a *linear programming problem*, where the equality and inequality constraints are imposed by the required shaper structure and properties.

In Cole and Wongratanaphisan (2011), analogously to Lim et al. (1999), a generalized FIR filter with shaping capability is proposed. By analysis of the FIR and the system convolution, the conditions on the smooth FIR function are derived. For a discrete shaper form, the designed task is turned to either linear or quadratic programming problem - the other providing the minimum quadratic gain. Note that the equality and inequality constraints are imposed by the performance and structural properties of the FIR filter, as discussed above for the shaper. Compared to lumped delay shapers, the impulse response has no singularities and as such, it filters discontinuities from a command input. The design methodology also allows to handle multiple modes within a single shaper design. The method was subsequently extended to adaptive input shaping by discrete FIR filter in Cole (2011) and Cole and Wongratanaphisan (2013). In Cole (2012) a fundamental set of input shaper design solutions was derived that give exact vibration cancellation for a finite number of modes and also have low-pass properties with a specified degree of high-frequency attenuation. H_2 optimal FIR pre-filter is proposed in Cole et al. (2018) for vibration suppression in machine motion control. A finite horizon optimization was adopted by Goubej and Helma (2019) for the derivation of an optimal open-loop control strategy for damping oscillations in gantry crane systems.

Recently, enhanced attention was paid to employing the optimization methods in design of distributed delay shapers. In Vyhlídal and Hromčík (2015), a method based on the constrained linear least squares optimization was proposed for direct design of robust shapers with piece-wise equally distributed delay. The residual vibration function was considered as the objective function. Consequently, in Pilbauer et al. (2017) the design task was addressed as a quadratic multi-objective problem balancing the robustness and the response time, i.e. two characteristics which are in conflict. The design of a shaper with piece-wise distribution of the delay was also targeted in Kungurtsev et al. (2017) where the stability constraint on the spectral abscissa was considered. The resulting non-smooth and non-convex optimization problem was then solved by SQP-GS algorithm, Curtis and Overton (2012).

3.3 Robust shaper design by quadratic programming

A most common optimization based shaper design method is by quadratic programming. Next to the lumped delay shaper (1), considering the pre-fixed values of the delays τ_i, let us consider the shaper with a piece-wise equally distributed delay described by the transfer function

$$S(s) = A_0 + \frac{1}{s}\sum_{i=1}^{n} A_i \mathrm{e}^{-s\tau_i}, \tag{13}$$

considering the delays $0 = \tau_1 < \tau_2 \ldots < \tau_n$ being equidistantly distributed over the pre-selected response time $T = \tau_n$, Vyhlídal and Hromčík (2015), Pilbauer et al. (2016).

The task to be targeted here is to optimize the single mode shapers with $S(s)$ given either by (1) or by (13). The oscillatory mode to be fully compensated is given by $r = -\omega\zeta - j\omega\sqrt{1-\zeta^2}$. The objective is to design a shaper robust against variations of the frequency ω considering the shaper action length $T = \tau_n$ and fixed number of delays to n. For both the shaper types, the parameters to be assessed are the gains

$$\mathbf{x} = [A_0 \; A_1 \;\; A_2 \; \cdots \; A_n]^\mathsf{T}. \tag{14}$$

The optimization problem can then be formulated as

$$\begin{array}{l} \min\limits_{\mathbf{x}} \;\; f(\mathbf{x}), \\ \text{subject to} \\ \begin{cases} A\mathbf{x} \geq b_1, \\ A_{eq}\mathbf{x} = b_2, \end{cases} \end{array} \tag{15}$$

where the equality and inequality constraints result from the performance and structural requirements on the shaper structure. A natural choice concerning the objective function $f(\mathbf{x})$ is to target the residual vibration function (10). Substituting the mode given by (ζ, ω) for s in the shaper transfer function $S(s)$, we obtain

$$S\left(-\omega\zeta - j\omega\sqrt{1-\zeta^2}\right) = L(\zeta, \omega)\mathbf{x} \tag{16}$$

with

$$L(\zeta, \omega) = \left[1 \; g_0(r) \cdots \; g_{N_p}(r)\right],$$

where $g_i = \mathrm{e}^{-s\tau_k}$ for (13) and $g_i = \frac{\mathrm{e}^{-s\tau_k}}{s}$ for (4), $i = 1..n$. Consequently, taking into account (10) we have

$$\begin{aligned} V(\zeta,\omega)^2 &= \mathbf{x}^\mathsf{T} \; L(\zeta,\omega)^* L(\zeta,\omega) \; \mathbf{x} e^{2\zeta\omega\tau_n} \\ &= \mathbf{x}^\mathsf{T} \; \Re(L(\zeta,\omega)^* L(\zeta,\omega)) \; \mathbf{x} e^{2\zeta\omega\tau_n} \end{aligned} \tag{17}$$

where $.^*$ denotes a complex conjugate transform. The robustness objective then can be formulated as minimizing $V(\zeta,\omega)^2$ over a region $\omega \in [\omega_{\min}, \omega_{\max}]$, with nominal frequency ω_{nom} assumed to be the midpoint of the interval. To handle the uncertainty in ω we define a grid of N_ω Chebyshev points, which are more efficient for polynomial approximation, Stewart (1996),

$$\omega_k = \left(\frac{\omega_{\max} + \omega_{\min}}{2}\right) - \left(\frac{\omega_{\max} - \omega_{\min}}{2}\right) \cos\left(\frac{(k-1)\pi}{N_\omega - 1}\right), \tag{18}$$

with $k = 1, ..., N_\omega$. Then the objective function can be formulated as

$$f(\mathbf{x}) = \frac{1}{N_\omega}\sum_{k=1}^{N_\omega} V(\zeta, \omega_k)^2. \tag{19}$$

By (17), the objective function is expressed by

$$f(\mathbf{x}) = \mathbf{x}^\mathsf{T} H \mathbf{x}, \tag{20}$$

where

$$H = \frac{1}{N_\omega}\sum_{k=1}^{N_\omega} e^{2\zeta\omega_k\tau_n} \Re\left\{L(\zeta,\omega_k)^* L(\zeta,\omega_k)\right\}. \tag{21}$$

The standard task for the *inequality constraints* is to ensure the non-negative character of the impulse response, leading to

$$A_i > 0 \tag{22}$$

for all the gains $i = 0..n$ for (4). For the distributed delay shaper (13), the inequality (22) is required only for $i = 0$. Then, the following inequalities are to be satisfied

$$-\sum_{k=1}^{l} A_k \leq 0 \text{ for } l = 1, 2, ..., n-1. \tag{23}$$

The primary task within the *equality* constraints is to impose the unity static gain of the shaper. For the lumped delay shaper (4), it leads to (2). For the distributed delay shaper (13), it leads to

$$\sum_{k=1}^{n} A_k = 0, A_0 - \sum_{k=1}^{n} A_k\tau_k = 1. \tag{24}$$

In order to compensate a specific oscillatory mode r entirely, a complex zero of the shaper is placed at the position of the oscillatory mode. Due to its complex nature, it leads to

$$\begin{cases} \Re(S(r)) = 0, \\ \Im(S(r)) = 0. \end{cases} \tag{25}$$

The entire procedure outlined above is fully described in Pilbauer et al. (2016) for the distributed delay shaper (13). In that paper, the problem was extended by considering uncertainties also in ζ and optimizing the shaper action time $T = \tau_n$ via modified objective function. It also included the software implementation and validation example.

4. CHANCE CONSTRAINED DESIGN BASED ON PROBABILITY DISTRIBUTIONS OF UNCERTAIN PARAMETERS

The interval uncertainty based design which include the minimax, EI, and SI class of Input Shapers, with lumped or distributed delays, only require knowledge of the support of the uncertainty. In numerous applications such as hard disk drives, one might gather enough samples of vibration characteristics of the read-write arms to generate a probability distribution function which can be exploited in the design of Input Shapers. Pao et al. (1997) considered uniform and Gaussian distribution for the uncertain parameters and formulated a cost function which is the expected value of the residual energy to determine the Input Shaper impulse sequence. Since minimizing the expected value alone does not correspond to reducing the variance, the resulting input shaper can lead to a residual energy distribution with a large variance which is undesirable. If higher moments of the distribution of the stochastic cost (Residual Energy) can be determined, they can be exploited to formulate performance metrics which are a function of the statistics of the stochastic cost. One popular approach for estimating the statistics of the evolving states and consequently the residual energy is generalized Polynomial Chaos (gPC), a popular approach for developing surrogate probabilistic models for a stochastic dynamical systems. The germ of the approach was first investigated by Norbert Wiener in his article Wiener (1938) where he approximated states of a Gaussian process with an infinite series expansion with Hermite polynomials as bases and called the approach Homogeneous Chaos. Subsequently, pioneering works by Cameron and Martin (1947), Ghanem and Spanos (1991) and Xiu and Karniadakis (2002) have resulted in significant progress of PC concepts. It has allowed for the development of surrogate models which can emulate the original stochastic system inexpensively and has been used to determine statistics (for example mean and variance) of states accurately.

Consider the linear state space model:

$$\dot{\mathbf{z}}(t,\xi) = A(\xi)\mathbf{z}(t,\xi) + B(\xi)\mathbf{u} \tag{26}$$

where $\mathbf{z} \in \mathbb{R}^{\tilde{n}}$, is the state vector which is a function of ξ, a vector of uncertain variables whose probability density function (pdf) is known.

From gPC theory, the states of the system in equation (26) can be expressed as

$$\mathbf{z}(t,\xi) = \sum_{i=0}^{\infty} \mathbf{z}_{:,i}(t)\Psi_i(\xi) \tag{27}$$

where, $\Psi_i(\xi)$ is a complete set of multivariate orthogonal (w.r.t the pdf of ξ) polynomials and $\mathbf{z}_{:,i} \in \mathbb{R}^{\tilde{n}}$ is the time varying coefficient vector (i.e. $\mathbf{z}_{:,i} = [z_{1,i} \, \dots \, z_{\tilde{n},i}]^T$) of $\Psi_i(\xi)$. Depending on the desired level of accuracy, typically the infinite series is truncated as an approximation:

$$\mathbf{z}(t,\xi) \approx \sum_{i=0}^{N} \mathbf{z}_{:,i}(t)\Psi_i(\xi). \tag{28}$$

The objective here in this modelling technique is to evaluate the unknown vectors $\mathbf{z}_{:,i}(t)$ over time. They can be determined by either intrusive methods or by non-intrusive methods, Kim et al. (2013). Intrusive methods require an analytical knowledge of the system model while non-intrusive methods can treat models as black boxes. In this development, since the models of interest are linear: the intrusive Galerkin projection is considered and investigated.

On substituting equation (28) in equation (26), we get

$$\sum_{i=1}^{N} \dot{\mathbf{z}}_{:,i}(t)\Psi_i(\xi) = A_z(\xi)\left[\sum_{i=0}^{N} \mathbf{z}_{:,i}(t)\Psi_i(\xi)\right] + B_z(\xi)\mathbf{u}(t). \tag{29}$$

Taking the Galerkin Projection of equation (29) over the basis function space, a deterministic system of equations is derived

$$M_{PC}\dot{\mathbf{Z}}_{\mathbf{PC}} = A_{PC}\mathbf{Z}_{\mathbf{PC}} + B_{PC}\mathbf{u}(t) \tag{30}$$

where $\mathbf{Z}_{\mathbf{PC}} = [\mathbf{z}_{:,0}^T, \mathbf{z}_{:,1}^T, ..., \mathbf{z}_{:,N}^T]^T$.

It has been well recognized that as the number of uncertain variables increase, the intrusive approach of generating the Polynomial Chaos based surrogate models which requires evaluation of high dimensional indefinite integrals, is computationally burdensome and is a drawback of intrusive polynomial chaos. Nandi and Singh (2019) demonstrated that for linear systems, using Lagrange interpolation function as the basis functions for gPC, one can generated a surrogate model by sample runs of the uncertain model, which exactly matches the surrogate model derived using the intrusive approach.

The moments of the states can now be estimated from the augmented state vector $\mathbf{z}_{:,i}(t)$:

$$\mathbf{E}[\mathbf{z}^m(t,\xi)] = \mathbf{E}[(\sum_{i=0}^{N} \mathbf{z}_{:,i}(t)\Psi_i(\xi))^m], \; i = 1, \dots, N. \tag{31}$$

For an orthogonal basis $\{\xi\}$ with $\xi_0 = 1$, the first two moments of the actual state vector $\mathbf{z}$ can be estimated analytically, as follows:

$$\mathbf{E}[z(t)] = \mathbf{E}[\sum_{i=0}^{N} \mathbf{z}_{:,i}(t)\Psi_i(\xi)] = \mathbf{z}_{:,0}(t) \tag{32}$$

$$\mathbf{E}[(\mathbf{z}(t) - \mathbf{z}_{:,0}(t))^2] = \sum_{i=1}^{N} c_i^2 \mathbf{z}_{:,i}^2(t) \tag{33}$$

where

$$\langle \Psi_i(\xi), \Psi_j(\xi)\rangle = \int_{\Omega} \Psi_i(\xi)\Psi_j(\xi)f(\xi)d\xi = c_i^2\delta_{ij}. \tag{34}$$

For precision motion control, the maneuver is often a rest-to-rest maneuver and, the residual energy at the end of the maneuver is a germane cost function. The residual energy at the final time t_f, which is a function of the uncertain parameter ξ can be defined as:

$$V(t_f,\xi) = \frac{1}{2}(\mathbf{z} - \mathbf{z_f})^T \begin{bmatrix} \mathbf{K} & \mathbf{0} \\ \mathbf{0} & \mathbf{M} \end{bmatrix} (\mathbf{z} - \mathbf{z_f}) \tag{35}$$

where $\mathbf{M}$ and $\mathbf{K}$ are the mass and stiffness matrices and the first half of the state vector $\mathbf{z}$ are the displacement states and the second half are the velocity states. $\mathbf{z_f}$ corresponds to the desired final states. If $\mathbf{K}$ is not positive definite, the cost function $V(t_f,\xi)$ has to be augmented with a quadratic term to ensure that the cost function is positive definite. The resulting cost function is:

$$V(t_f,\xi) = \frac{1}{2}(\mathbf{z} - \mathbf{z_f})^T \begin{bmatrix} \mathbf{K} & \mathbf{0} \\ \mathbf{0} & \mathbf{M} \end{bmatrix} (\mathbf{z} - \mathbf{z_f}) + \frac{1}{2}(z_r - z_{rf})^2 \tag{36}$$

where z_r refers to the rigid body displacement and z_{rf} is the desired final position.

The simplest cost function would be to minimize the mean of the residual energy:

$$J = \mathbf{E}[V(t_f,\xi)] = \int_{\Omega} V(t_f,\xi)f(\xi)d\xi \tag{37}$$

and a more general cost function which consists of a weighted sum of multiple moments of the residual energy, Singh et al. (2010):

$$J = \left(\alpha_1\mathbf{E}[V(t_f,\xi)] + \sum_{i=1}^{P} \alpha_i \left|\mathbf{E}[(V(t_f,\xi) - \mathbf{E}[V(t_f,\xi)])^i]\right|\right) \tag{38}$$

where $\alpha_i > 0$ are weighting parameters.

Preprints of the 21st IFAC World Congress (Virtual)
Berlin, Germany, July 12-17, 2020

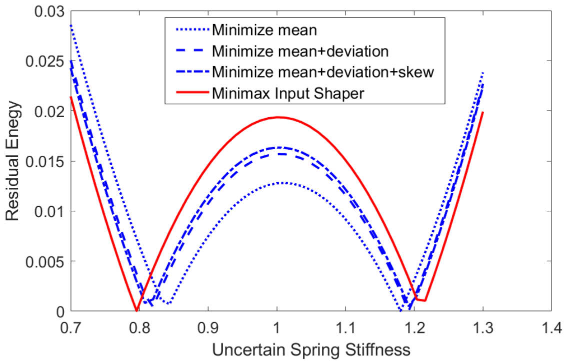

Fig. 3. gPC Uniform distribution (2 delays filter)

Consider the Input Shaper design for the undamped system:

$$m\ddot{x} + kx = ku \tag{39}$$

where k is a time-invariant uniformly distributed random variable over the range:

$$0.7 \leq k \leq 1.3. \tag{40}$$

and the mass is $m = 1$. The input-shaper/time-delay filter parameterized as:

$$S(s) = \sum_{i=0}^{2} A_i e^{-sT_i} \tag{41}$$

where $T_0 = 0$ and the parameters A_0, A_1, A_2, T_1 and T_2 is solved for to minimize statistics of the residual energy, with the constraint that $A_0 + A_1 + A_2 = 1$.

Solving the three-impulse Input Shaper (two time-delay filter) where the following cost functions were considered: i) the mean of the residual energy, ii) equally weighted mean and deviation of the residual energy, iii) equally weighted mean, deviation and cube root of the absolute value of the skew, results in optimal parameter listed in Table 1.

Figure 3 compares the performance of the gPC based design to the standard minimax controller design, which endeavors to minimize the maximum magnitude of the residual energy over the domain of spring stiffness uncertainty. It is clear from Figure 3 that as higher moments are included in the design process, the resulting solutions tend toward the minimax solution.

The Input Shapers described above either consider the nominal model and the sensitivity of the model to perturbations in the proximity of the nominal model, or consider the support of the uncertainty to pose a worst case design to develop robust controllers. One can imagine a scenario where a low probability realization of the uncertain vector drives the performance of the robust controller at the cost of not considering the high probability realizations of the uncertain vector. It is thus not difficult to motivate a problem where the user can specify a tolerable level of risk, which corresponds to a bound on the probability of violating a prescribed threshold of the cost, while minimizing the cost over the domain of the high probability space, Nandi and Singh (2017).

A probabilistic or chance constraint is represented by the equation:

$$P\left(h(x,\xi) \leq 0\right) \geq \eta \tag{42}$$

where $\eta \in [0,1]$ is the probability level, x corresponds to the decision variable(s) and ξ represents the random variable(s). For $\epsilon \in [0,1]$ representing the acceptable risk, Equation (42) can be rewritten as Calafiore and El Ghaoui (2006):

$$P\left(h(x,\xi) \leq 0\right) \geq 1-\epsilon. \tag{43}$$

For a linear chance constraints of the form:

$$P\left(\xi^T x \leq b\right) \geq \eta \tag{44}$$

where $\xi \sim \mathcal{N}\left(\bar{\xi},\Sigma\right)$, $\bar{\xi}$ and Σ are the mean and the covariance of the Gaussian random variable ξ respectively, we can represent:

$$P\left(\xi^T x - b \leq 0\right) = \Phi\left(\frac{b - \bar{\xi}^T x}{x^T \Sigma x}\right) \tag{45}$$

where Φ represents the cumulative distribution function of a normal distribution with 0 mean and unit variance. This permits rewriting the linear chance constraint as:

$$P\left(\xi^T x - b \leq 0\right) \geq \eta \Longleftrightarrow b - \bar{\xi}^T x \geq \Phi^{-1}(\eta)\,\|\Sigma^{1/2}x\|. \tag{46}$$

Equation (46) is a cone constraint and is convex for $\eta > 0.5$ Ben-Tal et al. (2009).

However, when the linear chance constraints is a function of a random variable whose pdf is not Gaussian or cannot be characterized by a well known pdf, the problem of imposing the exact chance constraint is challenging. This is often the scenario one encounters when imposing chance constraints on states of a dynamic system with uncertain model parameters. The issue, however, can be dealt with a robust version of the chance constraint as detailed below. Calafiore and El Ghaoui (2006) provide an approach to rewrite the linear probabilistic inequality:

$$P\left(\boldsymbol{\xi}^T \boldsymbol{x} + b \leq 0\right) \geq 1-\epsilon \tag{47}$$

where $\boldsymbol{\xi}$ and $\boldsymbol{x}$ are the vectors of random variables and decision variables respectively, as a convex deterministic constraint. In their work, they illustrate that if $\boldsymbol{\xi}$ and b are random variables with known means and variances, the constraint in equation (47) is equivalent to the convex constraint

$$\sqrt{\frac{1-\epsilon}{\epsilon}}\{var[\boldsymbol{\xi}^T\boldsymbol{x}+b]\}^{1/2} + E[\boldsymbol{\xi}^T\boldsymbol{x}+b] \leq 0 \tag{48}$$

where ϵ represents the risk level i.e. the probability with which the constraint is permitted to be violated. It should be noted that the constraint is conservative since it subsumes all distributions with the same mean and variance. Therefore, if only the first 2 moments of the random variables $(\boldsymbol{\xi}, b)$ are known, equation (48) allows one to enforce equation (47) no matter what the true distribution of $(\boldsymbol{\xi}, b)$ is. However, since this constraint is robust to all distributions, it can yields conservative solutions.

Consider the single spring-mass system whose dynamics are defined by Equation (39), where the mass of the system is $m = 5$ and k is a time-invariant uniformly distributed random variable over the range:

$$0.7676 \leq k \leq 1.2324. \tag{49}$$

Assuming an acceptable risk ϵ of 30%, which results in the probabilistic cost of minimizing the acceptable residual energy R:

$$P\left(V(t_f,k) \leq R\right) \geq 0.7 \tag{50}$$

Cost	A_0	A_1	A_2	T_1	T_2
$\mathbf{E}[V(T_2)] = \mu$	0.2545	0.4909	0.2545	3.1416	6.2831
$\mu + \sqrt{\mathbf{E}[(V(T_2) - \mu)^2]}$	0.2554	0.4892	0.2554	3.1416	6.2830
$\mu + \sqrt{\mathbf{E}[(V(T_2) - \mu)^2]} + \lvert\sqrt[3]{\mathbf{E}[(V(T_2) - \mu)^3]}\rvert$	0.2557	0.4886	0.2557	3.1415	6.2836

Table 1. Moment Based Optimal Input Shaper Design (2 Delays), Equation 38

which ensures that the probability of all realization satisfying the residual energy bound of R is greater than 70%. The maneuver time t_f is assumed be one period of the natural frequency of the system permitting the chance constrained design to be compared to the ZVD input shaper. Figure 4 illustrates the relative performance of the chance constrained Input Shaper design (solid blue line) to the ZVD shaper (red dashed line). Over the range of the uniformly distributed uncertain spring stiffness, the grey region illustrates the domain where any system realization will satisfy the required probabilistic threshold. The dark grey region is where the system realization do not satisfy the required threshold. The conservative nature of the resulting solution can be gauged from the 10.4% fraction of the uncertain domain not satisfying the required residual energy threshold when the acceptable risk was 30%. It is also clear from the figure that the performance of the Input shaper within the domain of acceptable risk is significantly better than the ZVD shaper's performance.

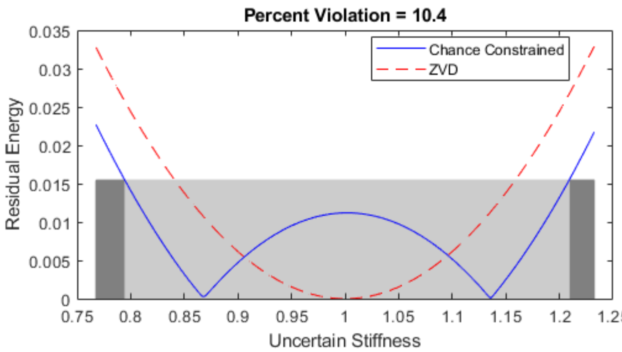

Fig. 4. Chance Constrained Input Shaper (2 delays filter), Equation 50

5. INPUT SHAPERS WITHIN FEEDBACK LOOPS

Besides reference shaping, input shapers have proven to be applicable within feedback loops. The motivation is mainly in extending the capability to pre-compensate the flexible modes responses induced by disturbances.

5.1 Shaper spectral properties

Before the overview and brief analysis of available feedback solutions, we point to spectral properties of the shaper zeros which play an important role once the shaper is placed within a feedback loop. First, consider the lumped delay shaper with the transfer function (4). Due to the exponential terms arising from the Laplace-transforms of the delayed variables, the equation

$$S(s) = A_0 + \sum_{i=1}^{n} A_i \mathrm{e}^{-s\tau_i} = 0 \tag{51}$$

has infinitely many roots, determining the shaper zeros. The function $S(s)$ in the form (51) corresponds to a characteristic function of a delay-difference equation, Hale and Lunel (1993). Such a function is known to have *neutral* spectrum of zeros r_i distributed in a vertical strip of the complex plane $\alpha < \Re(r_i) < \beta, \alpha \in \Re, \beta \in \Re$. As a consequence, the shaper can have infinitely many zeros close to the imaginary axis or even located to the right of the imaginary axis.

Considering the most common type of the distributed delay shaper (13), its zeros are determined by the equation

$$S(s) = A_0 + \frac{1}{s}\sum_{i=1}^{n} A_i \mathrm{e}^{-s\tau_i} = 0,$$

which has the same distribution of zeros as

$$\bar{S}(s) = A_0 s + \sum_{i=1}^{n} A_i \mathrm{e}^{-s\tau_i} = 0 \tag{52}$$

except $\bar{S}(s)$ has an additional root at the origin of the complex plane. Unlike for (51), the spectrum of $\bar{S}(s)$ zeros is *retarded*, Hale and Lunel (1993). With increasing magnitude of zeros, the zeros tend to depart to the left of the imaginary axis, following asymptotic exponential curves, Vyhlidal and Zítek (2009). Thus, as a consequence, the equation (52) has at most a finite number of right-half-plane zeros.

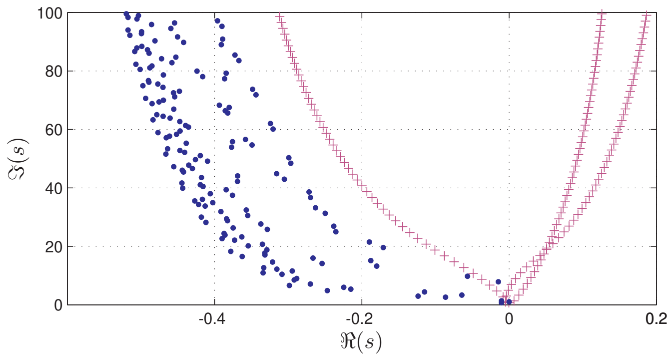

Fig. 5. Comparison of the retarded spectra of zeros (∘) of the distributed delay shaper (13) (Vyhlídal and Hromčík (2015)) with the neutral spectra of zeros (+) of Two-Hump EI shaper(Singhose et al. (1997))

Difference between spectrum distribution is demonstrated in Fig. 5, adopted from Vyhlídal and Hromčík (2015). The retarded spectrum of a distributed delay shaper is compared with neutral spectrum of a Two-Hump EI shaper designed in Singhose et al. (1997). Note that both the shapers have analogous residual vibration characteristics (see Fig. 8 of Vyhlídal and Hromčík (2015)). As can be seen, the Two-Hump EI shaper has many right-half plane zeros (in fact infinitely many due to spectrum periodicity). If the shaper is applied just for reference shaping as in Fig. 1, the distribution of shaper zeros have no effect on the closed loop stability. However, if the shaper is placed within the feedback loop, the distribution of the shaper zeros plays a significant role in the distribution of closed loop poles, Vyhlídal et al. (2016).

In what follows, the effect of a shaper on closed loop stability is outlined together with the ability of compensation of the flexible mode in responses to system output disturbance d_o and the sensor disturbance d_s. In the closed loop schemes, we assume that the main body of the system $G(s)$, which is controlled by the controller $C(s)$ is decoupled from the flexible subsystem $F(s)$ with the oscillatory modes to be compensated and for which the shaper is designed. Naturally, the most common scheme in Fig. 1 with the shaper outside the loop is ineffective in mode compensation induced by any of the disturbances.

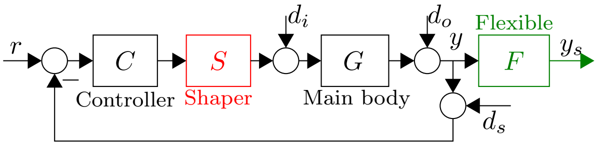

Fig. 6. Feedback interconnection with control input shaper

5.2 *Control input shaper*

The control scheme with the *control-input shaper* in Fig. 6 was analysed in Hung (2003). Closed loop stability issues related to this setup were discussed by Staehlin and Singh (2003) using root locus diagrams, and by Huey and Singhose (2009). In all these work, it is reported that the closed loop synthesis is considerably complicated due to time delays which are integral to the shaper. In Huey et al. (2008), it is shown that the architecture is effective in suppressing the sensor disturbances, but ineffective in suppressing the oscillations themselves as they are excited by the output disturbance. It is also shown in Huey et al. (2008) that the actuator saturation can be handled by the scheme in Fig. 6, if an *artificial* saturation (with the same threshold as the real saturation) is placed between the controller and the shaper.

From the sensitivity analysis, it results that

$$T_{y_s d_o}(s) = \frac{1}{1 + C(s)S(s)G(s)} F(s), \tag{53}$$

$$T_{y_s d_s}(s) = \frac{C(s)G(s)}{1 + C(s)S(s)G(s)} S(s)F(s). \tag{54}$$

As can be seen, the active zeros of $S(s)$ can compensate the effect of oscillatory pole of $F(s)$ only in the T_{y_s,d_s} transfer function, which shows its proper functioning in responses to sensor disturbance. However, for compensating the effect of output disturbance, which is more likely to happen in real applications, the scheme is not effective.The closed loop dynamics determined by the characteristic equation

$$1 + C(s)S(s)G(s) = 0 \tag{55}$$

is retarded for both the shaper types, except the case when both the controller and the system are bi-proper. In this case, the closed loop with the lumped delay shaper (4) is a neutral time delay system, Vyhlídal et al. (2016), with all the risky stability consequences. Before moving further, let us point to recently proposed SHAVO (SHAper + serVO) control scheme, Beneš et al. (2019), where the actuator control loop is used to correct the differences between true and modelled shaped outputs of the flexible system, including those induced by disturbances during the transient response.

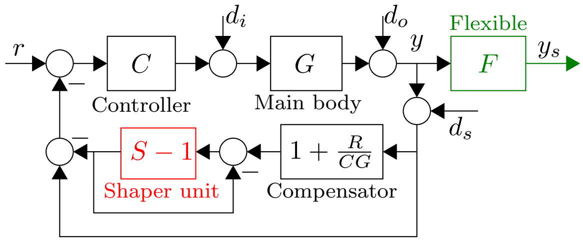

Fig. 7. Smith-like compensation scheme

5.3 *Smith's scheme with delay compensator*

The next scheme, shown in Fig. 7 originates from the scheme proposed already by Smith (1958). The slight modification towards extending its applicability was performed in Vyhlídal et al. (2016). The modified *Smith's scheme* has the sensitivity functions

$$T_{y_s d_o}(s) = \frac{1}{S(s)(1 - R(s)) + C(s)G(s) + R(s)} S(s)F(s) \tag{56}$$

$$T_{y_s d_s}(s) = \frac{C(s)G(s) - S(s)R(s) + R(s)}{S(s)(1 - R(s)) + C(s)G(s) + R(s)} F(s) \tag{57}$$

where $R(s)$ is a low-pass filter added to the Smith's scheme by Vyhlídal et al. (2016). As can be seen, the performance is converse to the scheme in Fig 6. Due to the term $S(s)F(s)$ in T_{y_s,d_o}, the mode can be compensated in responses induced by d_o. This is not however the case for the $d_s \to y_s$ channel. Due to the characteristic equation

$$S(s)(1 - R(s)) + C(s)G(s) + R(s) = 0 \tag{58}$$

the closed loop system is of neutral type for lumped delay shaper (4), whereas it is of more convenient *retarded type* for distributed delay shaper (13). Besides, for the roots with high magnitude, considering $C(s)G(s)$ is strictly proper, the roots of (58) tend to match the high-magnitude roots of $S(s) = 0$. Therefore, the application of lumped delay shaper (4) is rather risky from the stability perspective. For example, if the Two-Hump EI shaper with zeros distribution shown in Fig. 5 is applied, the closed loop system would have infinitely many unstable poles with high magnitude. On the other hand, the application of distributed delay shaper (13) does not bring such a stability risk. Thus, it should be preferred in the Smith's scheme.

Before proceeding further, let us discuss the purpose and properties of $R(s)$ filter. Note that in the original Smith's scheme $R(s) = 1$. This has positive consequences to the closed loop dynamics as the shaper transfer function $S(s)$ (with delay terms) is fully compensated in the denominators of the closed loop transfer functions. However, this can be applied if and only if both $C(s)$ and $G(s)$ are bi-proper, which is very unlikely in practice. The primary role of $R(s)$ is to make $\frac{R(s)}{G(s)C(s)}$ implementable if $C(s)G(s)$ is strictly proper. In order to preserve $S(s)$-compensation at the low frequency range, the cut-off frequency of the filter $R(s)$ should be considerably larger than ω.

5.4 Feedback inverse shaper

The last *inverse shaper* scheme shown in Fig. 8 was proposed by Vyhlídal et al. (2016). As can be seen from the sensitivity analysis

$$T_{y_s d_o}(s) = \frac{1}{S(s) + C(s)G(s)} S(s)F(s) \tag{59}$$

$$T_{y_s d_s}(s) = \frac{C(s)G(s)}{S + C(s)G(s)} F(s) \tag{60}$$

analogously to the Smith's scheme, the mode compensation takes place in the responses induced by d_o, but it does not in the responses induced by d_s. The characteristic equation

$$S(s) + C(s)G(s) = 0 \tag{61}$$

is neutral for the lumped delay shaper (4), and retarded for distributed delay shaper (13). In both cases the high magnitude roots tend to match the high magnitude zeros of the shaper. Thus, the application of distributed delay shaper is much safer from the stability perspective. Unlike in the *Smith's scheme*, the controller $C(s)$ design needs to be performed taking into consideration the infinite dimensionality of the closed loop. A controller design for the inverse shaper scheme by spectral optimization was proposed in Pilbauer et al. (2018).

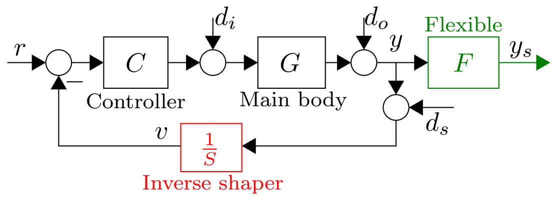

Fig. 8. Feedback interconnection of an inverse shaper according to Vyhlídal et al. (2016)

In the above schemes, no coupling was considered between the flexible subsystem and the main body. If this happens, the flexible mode can be deflected from the mode of the flexible part. A systematic approach to derive the flexible mode of the coupled system to be targeted by the inverse shaper was proposed by Hromčík and Vyhlídal (2017) and experimentally validated by Pilbauer et al. (2018).

Let us also point to the effect of the input disturbance d_i in the above analysed schemes. As $T_{y_s d_i}(s) = T_{y_s d_o}(s)G(s)$, the conclusions obtained for d_o apply also for d_i. In Alikoç et al. (2017) it was demonstrated that the inverse shaper functions well under the control saturation, which in some sense can be represented by the input disturbance. Concerning the shaper functioning in reference changes, because $T_{y_s r}(s) = T_{y_s d_o}(s)C(s)G(s)$ for Smith's and inverse-shaper schemes, and $T_{y_s r}(s) = T_{y_s d_o}(s)C(s)S(s)G(s)$ for the control input shaper scheme, the mode is compensated in all the considered schemes for this $w \to y_s$ channel.

6. CONCLUSIONS

The vast majority of interest in reference shapers has focused on those outside a feedback loop and some recent work has addressed the shaper design within the feedback loop. Minimal attention has been directed at the concurrent design of feedback controller and reference shapers. Preliminary work on second order systems has resulted in counter-intuitive results such as the need for the feedback controller to result in an undamped closed loop response since the reference shaper can eliminate the vibratory modes, and the lack of damping can reduce the transition time. Generalizing the design and incorporating uncertainties into the design is an area looking for attention.

Even though rudimentary attention has been paid to shaper performance under various non-linearities, further research is needed in this aspect. In the most common feed-forward layout, the linearity of the whole system is the key assumption for the oscillatory mode compensation. Most attention so-far has been paid to handling the actuator saturation. For the scheme in Fig. 6, it can be handled under slight adjustment of the scheme, Huey et al. (2008), whereas the inverse shaper schemes Fig. 8 handles the saturation effect directly, Alikoç et al. (2017). More attention needs to be paid to other constraints, such as limiting the actuator rate, acceleration and jerk. These can be embedded as constraints in the optimal design of the shaper. However, the complexity of optimal design can be restrictive for some applications. Further on, systematic attention should also be paid to the effects of dead-zone and friction phenomena.

In the optimal design, powerful convex optimizers are available for the shaper structure with prescribed delay lengths. This however often leads to enhanced demands on the compensator implementation. Approaches to achieve desired shaper performance under minimal parameterization in a convex programming framework are yet to be investigated. Concerning the shaper implementation within feedback loop, more attention should be paid to spectrum optimization due to the link to closed loop stability, Kungurtsev et al. (2017). For the closed loop shaper implementations, robust controller design is to be addressed in more detail taking into account infinite dimensionality of the closed loop. This leads to another challenging topic, which is targeting the shaper and the controller within a unified design framework. Another research direction is in applying the delays related to the oscillation period directly to the controller structure, Vyhlídal et al. (2017).

7. ACKNOWLEGEMENTS

The second author acknowledges support from the ESIF, EU Operational Programme Research, Development and Education, and from the Center of Advanced Aerospace Technology (CZ.02.1.01/0.0/0.0/16_019/0000826), Faculty of Mechanical Eng., Czech Technical University in Prague.

REFERENCES

Al-Numay, M.S. (2007). Unified approximate tracking control of linear systems with unacceptable zeros. *Journal of King Saud University-Engineering Sciences*, 19(2), 239–250.

Alikoç, B., Bušek, J., Vyhlídal, T., Hromčík, M., and Ergenç, A.F. (2017). Flexible mode compensation by inverse shaper in the loop with magnitude saturated actuators. *IFAC-PapersOnLine*, 50(1), 1251–1256.

Alikoç, B., Vyhlídal, T., and Ergenç, A.F. (2016). Closed-form smoothers and shapers with distributed delay for damped oscillatory modes. *IET Control Theory & Applications*, 10(18), 2534–2542.

Baumgart, M.D. and Pao, L.Y. (2007). Discrete time-optimal command shaping. *Automatica*, 43(8), 1403–1409.

Ben-Tal, A., El Ghaoui, L., and Nemirovski, A. (2009). *Robust optimization*. Princeton University Press.

Beneš, P., Valášek, M., Šika, Z., Zavřel, J., and Pelikán, J. (2019). Shavo control: the combination of the adjusted command shaping and feedback control for vibration suppression. *Acta Mechanica*, 230(5), 1891–1905.

Butterworth, J., Pao, L., and Abramovitch, D. (2012). Analysis and comparison of three discrete-time feedforward model-inverse control techniques for nonminimum-phase systems. *Mechatronics*, 22(5), 577–587.

Calafiore, G.C. and El Ghaoui, L. (2006). On distributionally robust chance-constrained linear programs. *Journal of Optimization Theory and Applications*, 130(1), 1–22.

Cameron, R.H. and Martin, W.T. (1947). The orthogonal development of non-linear functionals in series of fourier-hermite functionals. *Annals of Mathematics*, 48(2), 385–392. URL `http://www.jstor.org/stable/1969178`.

Cole, M.O. (2011). A discrete-time approach to impulse-based adaptive input shaping for motion control without residual vibration. *Automatica*, 47(11), 2504–2510.

Cole, M.O. (2012). A class of low-pass fir input shaping filters achieving exact residual vibration cancelation. *Automatica*, 48(9), 2377–2380.

Cole, M.O., Shinonawanik, P., and Wongratanaphisan, T. (2018). Time-domain prefilter design for enhanced tracking and vibration suppression in machine motion control. *Mech. Systems and Signal Proc.*, 104, 106–119.

Cole, M.O. and Wongratanaphisan, T. (2011). Optimal FIR input shaper designs for motion control with zero residual vibration. *Journal of Dynamic Systems, Measurement, and Control*, 133(2), 021008.

Cole, M.O. and Wongratanaphisan, T. (2013). A direct method of adaptive FIR input shaping for motion control with zero residual vibration. *IEEE/ASME Transactions on Mechatronics*, 18(1), 316–327.

Conord, T. and Singh, T. (2006). Robust input shaper design using linear matrix inequalities. In *2006 IEEE Conf. on Comp. Aid. Control Syst. Design, 2006 IEEE Int. Conf. on Control App., 2006 IEEE Int. Symp. on Intelligent Control*, 1470–1475. IEEE.

Curtis, F.E. and Overton, M.L. (2012). A sequential quadratic programming algorithm for nonconvex, nonsmooth constrained optimization. *SIAM Journal on Optimization*, 22(2), 474–500.

Ghanem, R.G. and Spanos, P.D. (1991). *Stochastic Finite Elements: A spectral Approach*. Springer New York.

Goubej, M. and Helma, V. (2019). Vibration damping in gantry crane systems: Finite horizon optimal control approach. In *2019 24th IEEE Int. Conf. Emerging Techn. and Factory Automation (ETFA)*, 877–882. IEEE.

Hale, J.K. and Lunel, S.M.V. (1993). *Introduction to functional differential equations*, volume 99. Springer Science & Business Media.

Hartmann, R. and Singh, T. (1999). Fuel/time optimal control of flexible structures: A frequency domain approach. *J. of Vibration and Control*, 5(5), 795–817.

Hromčík, M. and Vyhlídal, T. (2017). Inverse feedback shapers for coupled multibody systems. *IEEE Transactions on Automatic Control*, 62(9), 4804–4810.

Huey, J.R. and Singhose, W. (2009). Trends in the stability properties of clss controllers: a root-locus analysis. *IEEE Trans. on Control Systems Techn.*, 18(5), 1044–1056.

Huey, J.R., Sorensen, K.L., and Singhose, W.E. (2008). Useful applications of closed-loop signal shaping controllers. *Control Engineering Practice*, 16(7), 836–846.

Hung, J.Y. (2003). Feedback control with posicast. *IEEE Transactions on industrial electronics*, 50(1), 94–99.

Iamratanakul, D., Jordan, B., Leang, K.K., and Devasia, S. (2008). Optimal output transitions for dual-stage systems. *IEEE Transactions on Control Systems Technology*, 16(5), 869–881.

Kim, K.K.K., Shen, D.E., Nagy, Z.K., and Braatz, R.D. (2013). Wiener's polynomial chaos for the analysis and control of nonlinear dynamical systems with probabilistic uncertainties [historical perspectives]. *IEEE Control Systems*, 33(5), 58–67.

Kungurtsev, V., Pilbauer, D., Vyhlídal, T., Hromčík, M., and Michiels, W. (2017). Input shaper optimization with a constraint on the spectrum distribution. *IFAC-PapersOnLine*, 50(1), 13324–13329.

Lim, S., Stevens, H.D., and How, J.P. (1999). Input shaping design for multi-input flexible systems. *Journal of dynamic systems, measurement, and control*, 121(3), 443–447.

Liu, S. and Singh, T. (1997). Robust time-optimal control of nonlinear structures with parameter uncertainties. *ASME J. of Dynamic Systems, Measurement and Control*, 119(4), 743–748.

Meckl, P.H. and Arestides, P.B. (1998). Optimized s-curve motion profiles for minimum residual vibration. In *Proc. 1998 American Control Conference. ACC (IEEE Cat. No. 98CH36207)*, volume 5, 2627–2631.

Muenchhof, M. and Singh, T. (2003). Jerk limited time optimal control of flexible structures. *ASME Journal of Dynamic Systems, Measurement and Control*, 125(1), 139–142.

Murphy, B.R. and Watanabe, I. (1992). Digital shaping filters for reducing machine vibration. *IEEE Transactions on Robotics and Automation*, 8(2), 285–289.

Nandi, S. and Singh, T. (2017). Chance constraint based design of input shapers. In *2017 IEEE Conference on Control Technology and Applications (CCTA)*, 1757–1762. IEEE.

Nandi, S. and Singh, T. (2019). Nonintrusive global sensitivity analysis for linear systems with process noise. *J. of Computational and Nonlinear Dynamics*, 14(2).

Newman, D., Hong, S.W., and Vaughan, J.E. (2018). The design of input shapers which eliminate nonzero initial conditions. *Journal of Dynamic Systems, Measurement, and Control*, 140(10).

Pao, L.Y., Chang, T.N., and Hou, E. (1997). Input shaper designs for minimizing the expected level of residual vibration in flexible structures. In *Proceedings of the 1997 American Control Conference (Cat. No. 97CH36041)*, volume 6, 3542–3546. IEEE.

Peng, J., Huang, J., and Singhose, W. (2019). Payload twisting dynamics and oscillation suppression of tower cranes during slewing motions. *Nonlinear Dynamics*, 98(2), 1041–1048.

Perez, H. and Devasia, S. (2003). Optimal output-transitions for linear systems. *Automatica*, 39(2), 181–

192.

Pilbauer, D., Michiels, W., Bušek, J., Osta, D., and Vyhlídal, T. (2018). Control design and experimental validation for flexible multi-body systems pre-compensated by inverse shapers. *Systems & Control Letters*, 113, 93–100.

Pilbauer, D., Michiels, W., and Vyhlidal, T. (2016). Multi-criteria optimisation design of shapers with piece-wise equally distributed time-delay. *IFAC-PapersOnLine*, 49(10), 112–117.

Pilbauer, D., Michiels, W., and Vyhlídal, T. (2017). Distributed delay input shaper design by optimizing smooth kernel functions. *Journal of the Franklin Institute*, 354(13), 5463–5485.

Robertson, M.J. and Singhose, W.E. (2001). Multi-level optimization techniques for designing digital input shapers. In *American Control Conference, 2001. Proceedings of the 2001*, volume 1, 269–274. IEEE.

Schlegel, M. and Goubej, M. (2010). Feature-based parametrization of input shaping filters with time delays. *IFAC Proceedings Volumes*, 43(2), 247–252.

Singer, N.C. and Seering, W.P. (1988). Using acausal shaping techniques to reduce robot vibration. In *Proc. 1988 IEEE International Conference on Robotics and Automation*, 1434–1439. IEEE.

Singer, N.C. and Seering, W.P. (1990). Preshaping command inputs to reduce system vibration. *J. of dynamic syst., measurement, and control*, 112(1), 76–82.

Singh, T. (2002). Minimax design of robust controllers for flexible systems. *AIAA Journal of Guidance, Control and Dynamics*, 25(5), 868–875.

Singh, T. (2004). Jerk limited input shapers. *ASME Journal of Dynamic Systems, Measurement and Control*, 126(1), 215–219.

Singh, T. (2008). Minimax input shaper design using linear programming. *ASME Journal of Dynamic Systems, Measurement and Control*, 130(5), –.

Singh, T. (2012). Pole-zero, zero-pole canceling input shapers. *ASME Journal for Dynamic Systems, Measurement and Control*, 134(1).

Singh, T. and Vadali, S.R. (1994). Robust time-optimal control: A frequency domain approach. *Journal of Guidance, Control and Dynamics*, 17(2), 346–353.

Singh, T. (2009). *Optimal reference shaping for dynamical systems: theory and applications*. CRC Press.

Singh, T. and Singhose, W. (2002). Input shaping/time delay control of maneuvering flexible structures. In *Proceedings of the 2002 American Control Conference (IEEE Cat. No. CH37301)*, volume 3, 1717–1731. IEEE.

Singh, T., Singla, P., and Konda, U. (2010). Polynomial chaos based design of robust input shapers. *ASME J. for Dynamic Systems, Measurement and Control*, 132(5).

Singh, T. and Vadali, S. (1993). Robust time-delay control. *J. Dyn. Systems, Measur., Control*, 115(2A), 303–306.

Singh, T. and Vadali, S. (1995). Robust time-delay control of multimode systems. *Int. J. of Control*, 62(6), 1319–1339.

Singhose, W., Singh, T., and Seering, W. (1999). On-off control with specified fuel usage. *ASME Journal of Dynamic Systems, Measurement and Control*, 121(2), 206–212.

Singhose, W. (2009). Command shaping for flexible systems: A review of the first 50 years. *International journal of precision engineering and manufacturing*, 10(4), 153–168.

Singhose, W., Eloundou, R., and Lawrence, J. (2010). Command generation for flexible systems by input shaping and command smoothing. *Journal of guidance, control, and dynamics*, 33(6), 1697–1707.

Singhose, W., Seering, W., and Singer, N. (1994). Residual vibration reduction using vector diagrams to generate shaped inputs. *Journal of Mechanical Design*, 116(2), 654–659.

Singhose, W.E., Porter, L.J., Tuttle, T.D., and Singer, N.C. (1997). Vibration reduction using multi-hump input shapers. *Journal of dynamic systems, Measurement, and control*, 119(2), 320–326.

Singhose, W.E., Seering, W.P., and Singer, N.C. (1996). Input shaping for vibration reduction with specified insensitivity to modeling errors. *Japan-USA Sym. on Flexible Automation*, 1, 307–13.

Smith, O.J. (1958). *Feedback control systems*. McGraw-Hill.

Staehlin, U. and Singh, T. (2003). Design of closed-loop input shaping controllers. In *Proc. 2003 American Control Conference, 2003.*, volume 6, 5167–5172. IEEE.

Stewart, G.W. (1996). *Afternotes on numerical analysis*, volume 49. Siam.

Tallman, G. and Smith, O. (1958). Analog study of dead-beat posicast control. *IRE Transactions on Automatic Control*, 4(1), 14–21.

Tomizuka, M. (1987). Zero phase error tracking algorithm for digital control. *Journal of Dynamic Systems, Measurement, and Control*, 109(1), 65–68.

Tuttle, T.D. and Seering, W.P. (1994). A zero-placement technique for designing shaped inputs to suppress multiple-mode vibration. In *American Control Conference*, volume 3, 2533–2537. IEEE.

Van den Broeck, L., Pipeleers, G., De Caigny, J., Demeulenaere, B., Swevers, J., and De Schutter, J. (2008). A linear programming approach to design robust input shaping. In *Proc. 10th Int. Workshop on Advanced Motion Control*, 80–85.

Vyhlídal, T., Anderle, M., Bušek, J., and Niculescu, S.I. (2017). Time-delay algorithms for damping oscillations of suspended payload by adjusting the cable length. *IEEE/ASME Trans. on Mechatronics*, 22(5), 2319–2329.

Vyhlídal, T. and Hromčík, M. (2015). Parameterization of input shapers with delays of various distribution. *Automatica*, 59, 256–263.

Vyhlídal, T., Hromčík, M., Kučera, V., and Anderle, M. (2016). On feedback architectures with zero-vibration signal shapers. *IEEE Transactions on Automatic control*, 61(8), 2049–2064.

Vyhlídal, T., Kučera, V., and Hromčík, M. (2013). Signal shaper with a distributed delay: Spectral analysis and design. *Automatica*, 49(11), 3484–3489.

Vyhlidal, T. and Zítek, P. (2009). Mapping based algorithm for large-scale computation of quasi-polynomial zeros. *IEEE Trans. Automatic Control*, 54(1), 171–177.

Wiener, N. (1938). The homogeneous chaos. *American Journal of Mathematics*, 60(4), 897–936.

Xiu, D. and Karniadakis, G.E. (2002). The Wiener–Askey polynomial chaos for stochastic differential equations. *SIAM J. Sci. Comput.*, 24(2), 619–644.